New Absolute Cavity Pyrgeometer equation by application of Kirchhoff's law and adding a convection term

Bruce W. Forgan[1], Julian Gröbner[2], Ibrahim Reda[3]

[1]Docklands, Victoria, 3008, Australia
[2]PMOD/WRC, Davos Dorf, 7260, Switzerland
[3]NREL, Golden, Colorado, 80401-3393, USA

Correspondence to: Bruce W. Forgan (bwforgan@bigpond.com)

Abstract. An equation for the Absolute Cavity Pyrgeometer (ACP) is derived from application of Kirchhoff's law and the addition of a convection term to account for the thermopile being open to the environment unlike a domed radiometer. The equation is then used to investigate four methods to characterise key instrumental parameters using laboratory and field measurements. The first uses solar irradiance to estimate the thermopile responsivity, the second a minimisation method that solves for the thermopile responsivity and transmission of the cavity, and the third and fourth revisit the Reda et. al., 2012 linear least squares calibration technique. Data were collected between January and November 2020 when the ACP96 and two IRIS radiometers monitoring terrestrial irradiances were available. The results indicate good agreement with IRIS irradiances using the new equation. The analysis also indicates that while the thermopile responsivity, concentrator transmission and emissivity of an ACP can be determined independently, as an open instrument, the impact of the convection term is minor in steady state conditions but significant when the base of the instrument is being subjected to rapid artificial cooling or heating. Using laboratory characterisation of the transmission and emissivity, together with use of an estimated solar calibration of the thermopile generated mean differences of less than 1.5 Wm^{-2} to the two IRIS radiometers. A minimization method using each IRIS radiometer as the reference also provided similar results, and the derived thermopile responsivity was within 0.3 $\mu V/Wm^{-2}$ of the solar calibration derived infrared responsivity estimate of 10.5 $\mu V/Wm^{-2}$ estimated using a nominal solar calibration and provide irradiances within +/-2% of the terrestrial irradiance measured by the reference pyrgeometers traceable to SI. The calibration method using linear least squares regression introduced by Reda et al., 2012 that relies on rapid cooling of the ACP base but utilising the new equation was found to produce consistent results but was dependent on the assumed temperature of the air above the thermopile. This study demonstrates the potential of the ACP as another independent reference radiometer for terrestrial irradiance once the magnitude of convection coefficient and any potential variations in it have been resolved.

1 Background

Reda et al., 2012 introduced the Absolute Cavity Radiometer (ACP), its operational equations and characterization process. The ACP is an Eppley Laboratory pyrgeometer (PIR) with its dome replaced by a symmetrical cavity (called the concentrator)

internally coated by polished gold, and cooling/heating system attached to the base of the pyrgeometer to assist in cooling or heating the ACP body.

The Reda et al., 2012 derivation of the ACP equation uses a combination of radiative transfer but without consideration of reflected irradiance components and impacts of convection (Vignola et al., 2012). Blackbody calibration of an ACP has proven difficult and Reda et al., 2012 proposed a method of characterisation and calibration that included laboratory methods to determine the transmission of the concentrator and the emissivity of polished gold, while the thermopile sensitivity is determined using a linear least squares regression (LSQ) technique in the field at night under stable incoming irradiance conditions. Calibrations provided by Reda et al., 2012 assumed that the responsivity and transmission of the ACP changes over hours and days with variations of the order of several percent. More recently, Gröbner, 2021 has shown that the selection of points used in the field calibration have a significant influence on the result.

The ACP's body uses a Eppley Laboratory F3 thermopile which is used for Eppley Laboratory pyranometers (PSP) and pyrgeometers (PIR). The stability of F3 thermopile used for solar and infrared irradiance measurements in domed instruments is well within a percent over several years. Therefore, it was surprising to see the large variation in the ACP thermopile responsivity ($\mu V/(Wm^{-2})$) reported by Reda et al., 2012.

This paper derives a new ACP equation that adheres to Kirchhoff's law of thermal radiation for radiative transfer in vacuum and in-air measurements with a thermopile not protected by a dome and therefore includes an energy transfer term due to convection. The similarity and key differences in the contributing terms of the new in-air and the Reda et al., 2012 equations are also examined. Using the new equation, the impact on the laboratory characterisation, night-time calibration compared against two IRIS pyrgeometers, and an application of the linear LSQ methods are investigated.

2 **The steady-state equation for an ACP without a dome or concentrator in a vacuum**

An ACP without a concentrator is an Eppley Laboratory pyrgeometer without a dome that includes a thermistor to measure the temperature of the body. It has a flat thermopile receiver painted with Parsons Black. In a vacuum there is only radiative transfer between the source and the thermopile receiver, with no possibility of a convection component.

The ACP equation in this instance only involves Kirchhoff's law at the black surface of the thermopile receiver namely

$$1 = \alpha_r + \rho_r \quad (1)$$

where α_r is the fraction absorbed by the receiver which from Kirchhoff's law is equivalent to emissivity ε_r and ρ_r is the fraction reflected from the receiver as there is no transmission through the black receiver surface.

The net flux between the incoming and outgoing flux results in a temperature difference between the base and receiver of the thermopile generating a voltage that is proportional to the net flux. That is,

$$KV = F\downarrow - F\uparrow \quad (2)$$

where K is the responsivity of the thermopile in $Wm^{-2}\mu V^{-1}$, V is the voltage and $F\downarrow$ and $F\uparrow$ are the downward and upward radiant fluxes. The downward flux is made up of a single component the irradiance from the source W,

$$F\downarrow = W \tag{3}$$

The upward flux has two components, the emission from the surface and the reflection of the incoming flux, that is,

$$F\uparrow = \varepsilon_r W_r + (1-\varepsilon_r)F\downarrow \tag{4}$$

where ε_r is the emissivity of the receiver, and W_r is the blackbody irradiance from the receiver; ρ_r is equal to $(1-\varepsilon_r)$ as there is no transmission through the receiver surface. Solving the two simultaneous equations the result is

$$KV = F\downarrow - F\uparrow = W\varepsilon_r - W_r\varepsilon_r = \varepsilon_r(W - W_r) \tag{5}$$

which gives for W

$$W = \frac{K}{\varepsilon_r}V + W_r = K_r V + W_r \tag{6}$$

where K_r is the responsivity of the thermopile receiver or $K_r = K/\varepsilon_r$.

W_r is given by σT_r^4 where σ is the Stefan-Boltzmann constant and T_r is the temperature at the top of the reciever. As T_r cannot be measured directly at time t it is approximated by

$$T_r(t) = T_b(t) + V(t)S \tag{7}$$

where T_b is the ACP body temperature, S is calculated based on known values of the Seebeck coefficient for the thermopile junctions. If n is the number of junctions and ϖ is the efficiency of the thermopile, then

$$S = \frac{1}{S_0 n \varpi} \tag{8}$$

For the Eppley Laboratory F3 thermopile used in an ACP, with 56 copper-constantan junctions, S_0 is ~40 μV/K, and Reda et al., 2012 suggested ϖ~0.65 or 65% efficiency. $(T_r - T_b)$ is dependent on the net incoming irradiance and the thermal conductivity of the thermopile, while S is a property solely of the thermopile, and impacts directly on the thermopile responsivity. ϖ may vary due to the manufacturing process. During operation of an ACP the maximum expected $(T_r - T_b)$ is about 0.7 K. Reda et al., 2012 proposed S to be 7.044×10^{-4}. For a T_b = 273.15 K, and steady state conditions where V~-800 μV (corresponding to the net radiation exchange of the ACP with a cloud free sky), if S is in error by 20% the impact on W_r is about 0.7 Wm^{-2} and increases proportionally with V and T_b.

3 **The steady-state equation of an ACP with a symmetrical concentrator in a vacuum**

The concentrator is assumed to have symmetrical transmission, absorption, and backscatter characteristics. That is,

$$1 = \tau + \beta + \alpha \tag{9}$$

where τ is the transmitted fraction of the incoming irradiance through the concentrator, α is the fraction of the incoming irradiance absorbed by the concentrator and β is the fraction of the incoming irradiance reflected out of the concentrator. Being a symmetrical cavity, each component's magnitude will remain the same if irradiance enters either end of the concentrator.

The concentrator walls coated in gold have an emissivity (or absorptivity) of ε_c that is a property of the surface and independent of the incoming irradiance. The fraction of incoming irradiance absorbed by the concentrator, α, is a consequence of ε_c and the multiple reflection of incoming irradiance on the concentrator walls, hence $\alpha \geq \varepsilon_c$.

For an ACP in a vacuum, the incoming flux $F\downarrow$ at the receiver (at one end of the symmetrical concentrator) has three components, the transmitted incoming atmospheric irradiance τW, any emission from the walls of the concentrator with a blackbody irradiance of W_c, $\varepsilon_c W_c$, and the back reflectance towards the receiver of the flux from the receiver $\beta F\uparrow$ that is,

$$F\downarrow = \tau W + \varepsilon_c W_c + \beta F\uparrow \tag{10}$$

The outgoing flux from the receiver is made up of two components in Eq. (4), thus,

$$F\downarrow = \frac{\tau W + \varepsilon_c W_c + \beta\varepsilon_r W_r}{1-\beta(1-\varepsilon_r)} \tag{11}$$

Solving the two simultaneous equations results in

$$KV = F\downarrow - F\uparrow = \frac{\varepsilon_r(\tau W + \varepsilon_c W_c - (1-\beta)W_r)}{1-\beta(1-\varepsilon_r)} \tag{12}$$

As a result, the incoming irradiance transmitted by the concentrator is

$$\tau W = \frac{(1-\beta(1-\varepsilon_r)K}{\varepsilon_r} V + (1-\beta)W_r - \varepsilon_c W_c \tag{13}$$

And the required irradiance is

$$W = \frac{(1-\beta(1-\varepsilon_r)K}{\varepsilon_r \tau} V + \frac{(1-\beta)}{\tau} W_r - \frac{\varepsilon_c}{\tau} W_c \tag{14}$$

Note that Eq. (14) would be similar to the domed pyrgeometer equation by Philipona et al., 1995 if the latter used T_r instead of the thermopile base temperature, and the transmission and emission is that of a dome instead of an open cavity.

4 The steady-state equation of an ACP with a symmetrical concentrator in the atmosphere

In air, as the concentrator is open to the atmosphere, and convection effects are not minimized by a dome (Robinson, 1966, Kondratyev, 1969, Vignola et al., 2012), a convection term is required. The effective flux input to the receiver by convection is given by

$$F_{conv} = \gamma(T_{air} - T_r) \quad (15)$$

where γ is the convection coefficient that is dependent on T_{air} the temperature of the air at the surface of the receiver, water vapour content, wind speed and air pressure (Vignola et al., 2012. The equivalent version of equation (10) is,

$$F\downarrow = \tau W_{atm} + \varepsilon_c W_c + \beta F\uparrow + \gamma(T_{air} - T_r) \quad (16)$$

The outgoing flux from the receiver is made up of two components, identical to Eq. (4).

Solving the two simultaneous equations results in

$$\tau W_{atm} = \frac{(1-\beta(1-\varepsilon_r))K}{\varepsilon_r} V + (1-\beta)W_r - \varepsilon_c W_c + \gamma(T_r - T_{air}) \quad (17)$$

and replacing (1-β(1-ε_r))K/ε_r with K_1 the atmospheric irradiance is

$$W_{atm} = \frac{K_1}{\tau} V + \frac{(1-\beta)}{\tau} W_r - \frac{\varepsilon_c}{\tau} W_c + \frac{\gamma}{\tau}(T_r - T_{air}) = \frac{K_1}{\tau} V + W_{net} \quad (18)$$

where W_{net} represents the non-voltage irradiance components, and

$$K_1 = \frac{(1-\beta(1-\varepsilon_r))}{\varepsilon_r} K = \frac{1}{C}$$

and C is the effective responsivity of the thermopile receiver in μV/(Wm^{-2}). The only difference between Eq. (14) and Eq. (18) is the convection term F_{conv}. In a domed radiometer, as the sensor surface and air under the dome are at near equilibrium, the effects of convection are minimized and their inclusion in the flux balance of the thermopile is not used.

As there is no direct measure of the air temperature in the concentrator near the receiver surface, Reda et al., 2012 averaged the output of six temperature sensors embedded in the concentrator T_c to represent T_{air}.

5 Examining the laboratory determined coefficients

The emissivity of the polished gold-plated concentrator in APC95 was found by NIST measurements to be 0.0225. The transmission of the concentrator derived by Zeng et al., 2010 used Eq. (6) for measurements in a vacuum such that

$$\tau = \frac{(V_c K_1 + W_{rc})}{S_c} \Big/ \frac{(V_0 K_1 + W_{r0})}{S_0} \quad (19)$$

with subscripts *o* and *c* representing ACP measurements with the concentrator removed and with the concentrator in-place. They also assumed the emissivity of the concentrator has no impact on the numerator implying the emissivity of the concentrator was zero. S_c and S_o are the reference output signals of the irradiance source; the derived value was 0.92. Reda et al., 2012 indicated that the K_1 value used by Zeng et al., 2010 was incorrect and used a value K_1~0.080 μV Wm^{-2}μV^{-1} (or C~12.5 μV/(Wm^{-2})) from field calibrations to generate a τ~0.993.

As these measurements were conducted in air and the concentrator emissivity is greater than zero, Eq. (18) applies and hence a convection term and concentrator emission term should have been added to the concentrator emissivity term in the numerator and the convection term in both the numerator and denominator, namely,

$$\tau = \frac{(V_c K_1 + W_{rc} - \varepsilon_c W_{cc} + \gamma(T_{rc} - T_{airc})}{S_c} \Big/ \frac{(V_0 K_1 + W_{r0} + \gamma(T_{ro} - T_{airo})}{S_0} \quad (20)$$

The laboratory setup used by Zeng et al., 2010 included a 10 μm laser and its irradiance was higher than the irradiance from base of the ACP, hence positive signals resulted from the ACP thermopile and T_r would have been higher than T_c. Setting β~0, ε_c=0.0225, and γ~8.5 and assuming the thermopile to air temperature difference was about +0.3 K in steady state conditions resulted in a 1.5% reduction in the transmission giving ~0.977 when compared to the values used in Reda et al., 2012. The impact of a zero contribution from the convection term decreased the derived transmission by less than 0.001.

Reda et al., 2012 utilised Eq. (19) and the results from Zeng et al., 2010 to derive a value of τ for each measurement sequence after updating K_1 via a linear LSQ calibration run. As a result, τ was deemed a function of K_1, rather than a unique characteristic of the concentrator.

For the remainder of this paper 0.977 will be used as the transmission of the concentrator.

6 Comparing the terms between the original and new ACP equations

Using the symbols above, the Reda et al., 2012 equation for incoming irradiance is

$$W_{atm} = \frac{K_1}{\tau} V + \frac{(2-\varepsilon_c)}{\tau} W_r - \frac{(\varepsilon_c + \varepsilon_{cav})}{\tau} W_c = \frac{K_1}{\tau} V + \frac{(2-\varepsilon_c) W_r - (\varepsilon_c + \varepsilon_{cav}) W_c}{\tau} \quad (21)$$

with the only additional term being the emissivity of the air in the cavity ε_{cav} which Reda et al., 2012 set to 1. Rearranging the terms, we have

$$W_{atm} = \frac{K_1}{\tau} V + \frac{1}{\tau} W_r - \frac{\varepsilon_c}{\tau} W_c + \frac{1}{\tau}(W_r - W_c) - \frac{\varepsilon_c}{\tau} W_r \quad (22)$$

The first 3 terms of Eq. (18) and Eq. (22) are identical if the concentrator backscatter β is zero. The latter two terms are where significant differences to the new equation exist. The (W_r - W_c) term is a difference between irradiances rather than a difference in temperatures in Eq. (18). In steady state conditions with the base of the ACP not subject to artificial cooling or heating, $W_r \leq W_c$ and -0.6< (T_r-T_c) ≤ 0.0, there is a relatively simple relationship between the irradiance difference and the temperature difference, namely

$$(W_r - W_c) \sim \psi (T_r - T_c) \quad (23)$$

where $\Psi \cong 5 \pm 2$ depending on the usual range of irradiance terms. The magnitude of γ from black body investigations using ACP96 is γ~8.4 and 6.5 depending on the blackbody configuration and are higher than Ψ. In essence, the (W_r - W_c) is a lower

magnitude version of the convection term in the new equation. The last term in Eq. (22), namely $-W_r\varepsilon_c/\tau$ adds a negative irradiance contribution due to the concentrator emissivity but sourced from the thermopile irradiance; this is not consistent with Kirchhoff's law as it adds emission from the concentrator walls other than due to the concentrator's temperature.

Hence the only differences between Eq. (22) and Eq. (18) are that for Eq. (22):
(a) the ε_c/τ terms have approximately double the contribution to the derived atmospheric irradiance; and
(b) the $(W_r - W_c)$ term could be slightly less in magnitude compared to the $\gamma(T_r - T_c)$.

The doubling of the ε_c/τ contribution in Eq. (22) impacts directly on any derivation of K_1 as it increases the negative contributions from both the concentrator and thermopile irradiance emission. That is, given V is normally negative and as the concentrator emissivity ε_c is a constant, the Reda et al., 2012 derived K_1 will be smaller (and hence C is larger) compared to Eq. (18) derivations by about 8%.

7 ACP calibration methods to date

As the ACP was developed to be an absolute radiometer that did not require calibration through comparison to another pyrgeometer or black body source, Reda et al., 2012 developed an innovative calibration method using linear LSQ that relies on periods of constant W_{atm} together with rapid changes in the thermopile base temperature. The base and concentrator temperature provides irradiance traceability to SI. As the calibration process rapidly and continuously drops the base temperature of the ACP the changes in signals and component irradiances are used to generate a linear LSQ regression solution. Two parameters are derived from the linear LSQ calibration process, $<K_1>$and $<\tau W_{atm}.>$. For Reda et al., 2012 ε_c and ε_{cav} coefficients in Eq. (22) are based on laboratory measurements or assumptions from literature.

To provide data for the Reda et al., 2012 linear LSQ process the ACP body is rapidly cooled over a set period. The rapid change in base temperature is required to minimize the risk that W_{atm} changes significantly over the cooling period. The measurements during the rapid heating after a cooling process are not used.

Using ACP96 data Gröbner, 2021 examined the linear LSQ process using the equation from Reda et. al. 2012 and developed procedures to remove the influence of the initial and final transient values and only used those data where a continuous cooling process is evident. The Gröbner, 2021 processing generated $<K_1>$ approximately 6% less that of the Reda et al., 2012 implementation.

Black body methods have been used successfully for decades to calibrate domed pyrgeometers and solving for Eq. (14) equivalents that have shown high levels of stability over several years (Gröbner and Wacker, 2012). In black body calibrations of a pyrgeometer, the base and dome temperatures of the pyrgeometer, and the black body output irradiance are changed independently and allowed to stabilize at set values. The data from this process allows a multivariant solution by LSQ

optimization methods. However, the final determination of K_1 is typically by using non-thermopile coefficients derived from the black body calibration together with a reference irradiance during night-time measurements (Gröbner and Walker, 2012).

Eq. (18) assumes $T_{air} \sim T_c$ and this maybe the reason standard black body methodologies (Gröbner and Walker, 2012) have not been successful for calibration of an ACP to date. The differences between a typical pyrgeometer and ACP are the replacement of a dome with the open concentrator, and the careful matching of the thermistors with the latter an improvement on normal pyrgeometer thermometry. The black body calibration process used for pyrgeometers requires a fixed number of temperature and black body stable temperature points that approximate atmospheric irradiances. Using a standard black body pyrgeometer calibration sequence the ACP thermopile and concentrator cavity are exposed to the air in the black body, and the black body is cooled to several temperature points well below the ACP body temperature. As a result $T_c << T_b$, and it is highly likely that $T_{air} << T_c$.

7.1 The impact of uncertainty in concentrator, thermopile and convection coefficients on W_{atm}

Using the new equation, the concentrator properties required are the concentrator transmission τ, its emissivity ε_c, the concentrator backscatter β, and the convection term is γ.

A value for the thermopile emissivity ε_r is not required as it is a constant and it is incorporated in K_1 (and C). For Parsons Black at terrestrial irradiance wavelength ε_r is ~0.92 and at solar wavelengths ~0.98. ε_r only becomes relevant if C is determined at solar wavelengths (C_{solar}), and then converted to a terrestrial irradiance value, as we will see below.

For ACP95 the concentrator emissivity was measured by NIST (Reda et al., 2012) and was found to be 0.0225 which is within 0.0015 of other known values for the emissivity (and hence absorptivity) of polished gold.

The impact of the irradiance backscatter fraction β and the receiver emissivity ε_r is minimal. Using the Zeng et al., 2010 transmission measurements and the new equation suggest that for a concentrator transmission τ greater than 0.9, and hence $(1-\tau) \geq \beta$ and $\varepsilon_r > 0.9$, then $(1-\beta(1-\varepsilon_r)) \geq 0.99$ and are essentially constant. Hence uncertainties in β and ε_r have little impact when incorporated into K_1.

The greatest potential impact due to concentrator transmission τ and backscatter β is on the W_r term where $1.1 \geq (1-\beta)/\tau > 1.0$ when the fraction of incoming irradiance absorbed by the concentrator α_c is greater than zero. If there is no absorption of the incoming irradiance by the concentrator (ie. $\alpha_c=0$) then $(1-\beta)$ is equal to τ. If $\alpha_c > \varepsilon_c$ given the NIST measurements and the Eq. (20) derivation of $\tau \sim 0.977$ and $\varepsilon_c \sim 0.0225$, that necessitates $\beta \leq 0.005$ if $\alpha_c = \varepsilon_c$. As $\beta \rightarrow 0$, any error in concentrator transmission will dominate the error contribution to W_{atm}.

The convection coefficient γ is problematic for several reasons. Firstly, at present it needs to be derived assuming the other coefficients or by approximation. Secondly it is dependent on the air flow, air temperature, relative humidity, and air pressure

at the surface of the thermopile receiver. The empirical evidence from blackbody and atmospheric measurements suggests $6<\gamma<10$.

The receiver temperature T_r and hence blackbody irradiance W_r are dependent on the estimate of the Seebeck coefficient and the construction of the thermopile and the measurement of the base temperature T_b. As the thermistors in an ACP have been characterised, Reda et al., 2012 estimated that the standard uncertainty in the W_r and W_c at about 0.1 Wm^{-2} and the standard uncertainty in the estimation of the Seebeck coefficient for the thermopile provides an additional 0.1 Wm^{-2} uncertainty contribution to W_r.

T_r is calculated using equation (7) on the assumption that the efficiency of the thermopile is as stated in Reda et al., 2012 and T_b is equivalent to the thermopile base temperature. K is also dependent on the Seebeck coefficient of the copper-constantan, the efficiency of the thermopile, the emissivity of the receiver surface ε_r and the conductivity of the thermopile. Incorrect assignment of the true Seebeck coefficient S in Eq. (7) will impact on two terms in Eqs. (18) and (22). However, S has not been derived for individual ACP, so the Reda et al., 2012 value will be assumed for this paper.

For solar wavelengths the emissivity of Parson's Black changes as the paint discolours over time due to solarization but has little if any impact on the IR emissivity.

Based on the above assumptions the components of uncertainty of a single measurement of W_{atm} using Eq. (18) are provided in Table 1. The dominant uncertainty components are K_1 and ε_c for the calculation of τW_{atm} and the standard uncertainty for both τW_{atm} and τ make similar contributes to the uncertainty of W_{atm}.

Table 1. The standard uncertainty calculation for W_{atm} = 289.33 Wm^{-2} by calculation by Eq. (18). The first 11 component rows provide the calculation of the standard uncertainty for τW_{atm}, while the remaining rows provide the calculation of the standard uncertainty for $W_{atm.}$ Apart from irradiance components (W_x) and dimensionless quantities ε_c and τ, the units of the components are provided in the first column.

Component x	Value	dx (u_{66})	dW/dx	dx*dW/dx	$(dx*dW/dx)^2$
τW_{atm}					
U (μV)	-750	1	0.0950	0.0950	$9.025x10^{-3}$
K_1 (Wm^{-2}/μV)	0.0950	0.0190	-750	-1.425	2.030
W_r	363.43	0.1	1	0.1027	$1.056x10^{-2}$

W_c	364.46	0.1	0.0225	$2.317x10^{-3}$	$5.367x10^{-6}$
ε_c	0.0225	$2.25x10^{-3}$	364.46	0.8200	$6.726x10^{-1}$
γ (Wm^{-2}/K)	6.5	1.5	-0.2000	-0.300	$9.000x10^{-2}$
T_r (°C)	9.80	0.02	6.5	0.13	$1.690x10^{-2}$
T_c (°C)	10.00	0.02	6.5	0.13	$1.690x10^{-2}$
				$\Sigma(dx*dW/dx)^2$	2.846
			τW_{atm}	Std. Uncertainty	1.687
W_{atm}					
τ^{-1}	1.0235	5.265x10-3	282.68	1.488	2.215
τW_{atm}	282.68	1.687	1.0235	1.727	2.982
				$\Sigma(dx*dW/dx)^2$	5.197
			W_{atm}	Std. Uncertainty	2.280

8 New Calibration Methods

Four calibration methods will be examined below for ACP96 based at PMOD/WRC in Davos, Switzerland, using either characterisation data, comparison measurements with other reference IRIS pyrgeometers, and implementing two versions of linear LSQ.

Based on the likely magnitude of the uncertainties, assumed values for some parameters are used in all the calibration methods investigated below. The value of the cavity emissivity is fixed at 0.0225 using the NIST derived value in Reda et al., 2012 for ACP95. The value for the backscatter from the concentrator β will be assumed to be 0.

Using black body investigations, two values of the convection coefficient have been estimated, 8.4 and 6.5. The latter value 6.5 derived from early blackbody investigations and field measurements produces convection-based irradiances closer to the

equivalent 'air cavity' irradiance values used by Reda et al., 2012. The logic behind this adjustment is not solely due to the convection coefficient being different, but rather the approximation $T_c \sim T_{air}$.

This leaves the sensitivity of the thermopile K_1 and the concentrator transmission τ to be either assumed or provided by a characterisation methodology.

For work reported below the transmission of the concentrator τ is assumed to be only due to the construction of the concentrator and is independent of K_1. The values of τ for ACP95 derived by the reanalysis of the Zeng et. al. (2010) data set but using Eq. (20), will be used when not derived as part of a calibration process.

The fraction of incoming terrestrial irradiance absorbed by the concentrator α_c is not independent of the concentrator ε_c. Concentrator transmission is a function of the cosine response of the concentrator and ray tracing suggests that for most sky zenith angles there will be multiple reflections on its surface, then $\alpha_c > \varepsilon_c$. For ε_c=0.0225 derived by NIST as reported by Reda et al., 2012, then the implication is that $\tau < 0.9775$.

For the results below when the method requires a fixed value of concentrator transmission τ is set to 0.977, and a fixed estimate of ε_c = 0.0225 and two values of the convection coefficient γ (8.4 and 6.5).

8.1 Data Sets

During 2020 there were 242 days of ACP96 data collected at PMOD/WRC and sometimes coincidentally with days IRIS4 and or IRIS2 data were collected. Night-time data were available from ACP96 and IRIS2 between 7 January 2020 and 10 December 2020, and between 15 March and 10 December for IRIS4. The data consisted of an average value every 60 seconds for any IRIS irradiance and a 1 s measurement sequence every 10 seconds for ACP96. Simultaneous measurements were available in 2020 with 41days of IRIS2 data and 36 days of IRIS4 that could be compared to ACP96.

Figure 1 shows a Box-Whisker representation of the differences between the simultaneous measurements of atmospheric terrestrial irradiances W_{IRIS2} and W_{IRIS4}. The typical daily range in differences is 1.5 Wm^{-2} which is within the individual instrument expanded uncertainty (k=2) of 2 Wm^{-2} (Gröbner, 2021). Slightly larger differences, with IRIS2 lower than IRIS4, are observed on two days in August (day of year 233 and 234), which are still within the combined uncertainties of the two radiometers. There appears to be a trend in the daily mean differences until day 260 and then a restoration of the early 2020 mean daily differences after day 300.

While there appears to be a drift between the two data sets it was decided to use both data sets as a reference or comparison data set. These IRIS data tested the impact of using different reference irradiances and were used to corroborate the results of the methods described below.

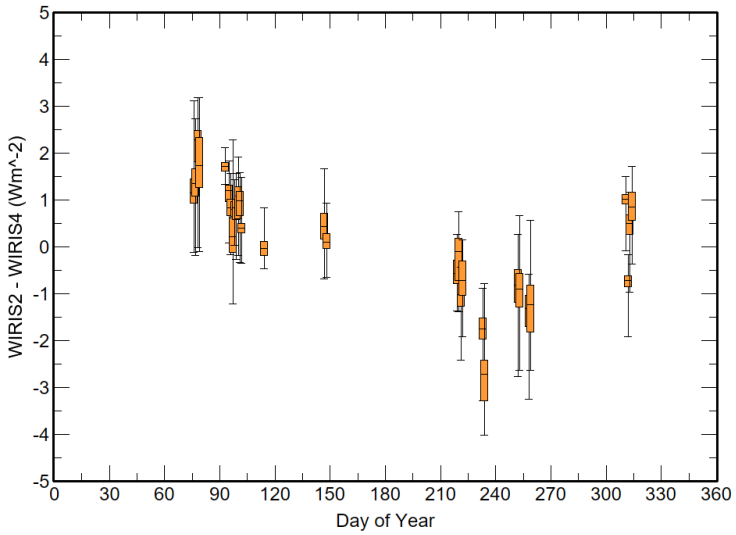

Figure 1. Statistics for the difference between W_{IRIS2} and W_{IRIS4} for every simultaneous irradiance in 2020 in Box-Whisker plots.

8.2 Deriving K_1 or C from an estimated solar calibration of the thermopile

For this method either prior to an ACP being assembled or by removing ACP's concentrator, the concentrator would be replaced with a pyrheliometer aperture system that conforms to pyrheliometer requirements, with the closest aperture to the receiver surface being identical to the aperture of the concentrator. The ACP would be pointed at the Sun and compared to a well calibrated WRR (or SI) pyrheliometer to produce an estimate of the thermopile responsivity to solar irradiance. That estimate would then be converted to the infrared responsivity by assuming the emissivity of the receiver surface for both solar (ε_{rsolar}) and infrared emission (ε_r).

Unfortunately, no solar calibration exists for the thermopile of ACP96 so an estimate had to be made and we will assume the ACP thermopile responsivity for solar irradiance, C_{solar}, would likely be that of a new F3 thermopile and use the calibrations of new PSP pyranometers were used to estimate a likely solar calibration for a F3 used an ACP. The data from over 82 individual PSP calibrations sourced from Eppley Laboratory and multiple national calibration centres in the USA, Canada and Australia indicated that the mode and mean solar sensitivities of new PSPs manufactured after 2000 was ~9.3 µV/(Wm^{-2}).

An estimate for C is the effective responsivity of the thermopile receiver in µV/(Wm^{-2}) is then,

$$C = \frac{\varepsilon_r C_{solar}}{\tau_{dome}^2 \varepsilon_{rsolar}} \quad (24)$$

As Parsons Black is used to coat the receiver surface, with a typical receiver solar emissivity ε_{rsolar} ~ 0.98 and for infrared ε_r ~

0.92, and a PSP has a double dome with both domes having a nominal transmission at solar wavelengths of τ_{dome} ~ 0.91, then this gives an estimate of C ~ 10.5 μV/ (Wm^{-2}).

Using the Eq. (18), the atmospheric irradiance W_{APC96} was calculated when both IRIS4 and IRIS2 were operating and ACP96 was monitoring in steady state night-time conditions. This resulted in comparisons over 41 nights (18802 measurements) with IRIS2 and 33 nights (14085 measurements) with IRIS4. The results are presented in Table 2 using C=10.5, γ=8.4, τ=0.977 and ε_s=0.0225; the daily mean differences (W_{IRIS2}- W_{ACP96}) and (W_{IRIS2}- W_{ACP96}) for each of the days are shown in Figure 2. Similar statistics are presented in Table 2 and figure 3 using γ = 6.5.

Table 2. The mean differences and the statistics of (W_{IRIS2}- W_{ACP96}) and (W_{IRIS4}- W_{ACP96}) in Wm^{-2} for data from January to November 2020, using C=10.5, γ=8.4, τ=0.977 and ε_s=0.0225.

	Number	Average	Std Deviation	Maximum	Minimum
W_{IRIS2}- W_{ACP96}	18802	0.23	1.21	2.64	-3.70
W_{IRIS4}- W_{ACP96}	14085	-0.18	0.88	2.03	-2.54

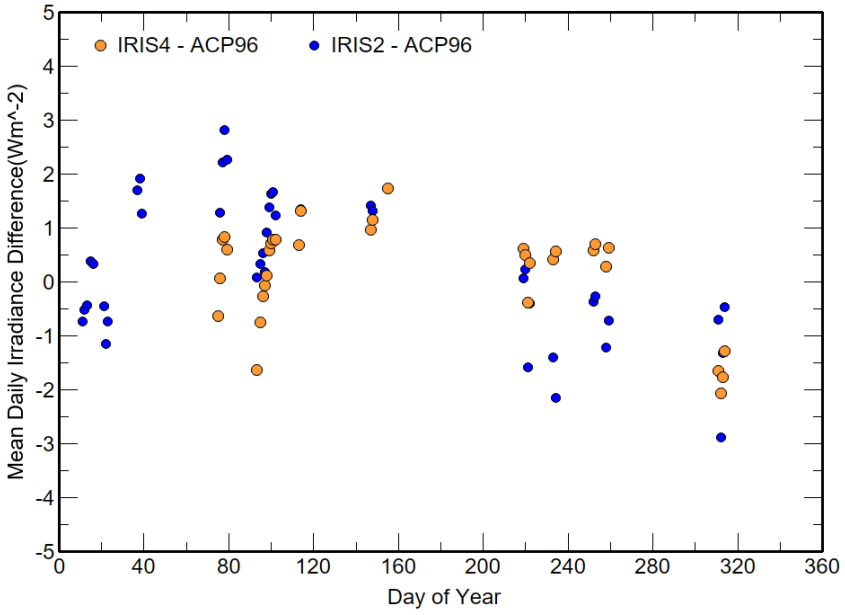

Figure 2. The daily mean differences and the statistics of (W_{IRIS2}- W_{ACP96}) and (W_{IRIS4}- W_{ACP96}) in Wm^{-2} from January to November 2020, using C=10.5, γ=8.4, τ=0.977 and ε_s=0.0225.

Table 3. The mean differences and the statistics of (W_{IRIS2} - W_{ACP96}) and (W_{IRIS4} - W_{ACP96}) in Wm^{-2} for data from January to November 2020, using C=10.5, γ=6.5, τ=0.977 and ε_c=0.0225.

	No	Mean	Std Deviation	Maximum	Minimum
W_{IRIS2}- W_{ACP96}	18802	-1.07	1.44	2.54	-5.55
W_{IRIS4}- W_{ACP96}	14085	-1.26	1.08	1.14	-4.71

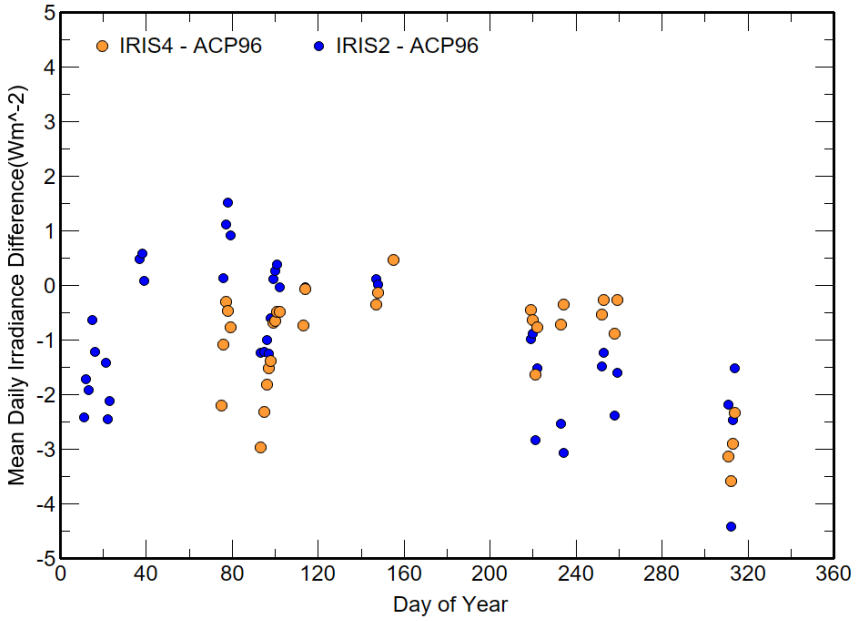

Figure 3. The daily mean differences and the statistics of (W_{IRIS2} - W_{ACP96}) and (W_{IRIS4} - W_{ACP96}) in Wm^{-2} from January to November 2020, using C=10.5, γ=6.5, τ=0.977 and ε_c=0.0225.

The differences to W_{IRIS2} were larger than for W_{IRIS4}, and there appears to be a similar trend in the relationship between IRIS2 and ACP96, as seen with the comparison between W_{IRIS2} and W_{IRIS4}. The differences between Table 2 and Table 3 shows the impact of a 22% change in γ for steady state conditions is 0.6 Wm^{-2} APC96 irradiance difference for a $\Delta\gamma$ = 1. Decreasing γ by -1.9 shifted all the mean values down by ~1.2. Wm^{-2} but increased the range of the W_{IRIS2}-W_{ACP96} while the W_{IRIS4}-W_{ACP96} showed little change.

8.3 Outdoor calibration using a reference irradiance

This method also assumes fixed values for the concentrator emissivity ε_c, and convection coefficient γ and finds the minimum difference between the reference irradiance W_{IRIS2} or W_{IRIS4}, and W_{ACP96} using paired values of K_1 and concentrator transmission τ. That is, for a set of n observations made up of m nights ideally with ranges in W_{IRIS} and W_{ACP96}, the pair [C, τ] is found that provides a mean difference of (W_{IRIS} - W_{ACP96}) of less than 0.1 Wm^{-2}. Given the low irradiance impact of concentrator emissivity, and convection coefficient in steady state conditions, the convergence to a solution is straight forward.

In the γ =8.4 set the (W_{IRIS}-W_{ACP96}) statistics for simultaneous measurements with IRIS2 and IRIS4 observations are presented in Table 4. There are differences of 0.4 (or ~4%) between the C values and 0.011 (~1.2%) between the resultant concentrator transmission values. The table also presents the results of using the average of the two C and transmission values derived from IRIS2 and IRIS4 giving C=10.5 and τ=0.9764 and deriving the difference statistics to both IRIS2 and IRIS4.

Table 4. The statistics of (W_{IRIS}-W_{ACP96}) using ε_c=0.0225 and γ=8.4 from March to November 2020, for the pairs of C and τ, that minimized the mean difference of W_{IRIS}-W_{ACP96}. The difference statistics using the average C and τ of the IRIS2 and IRIS4 results are also given in the last two rows of the table.

	No	*ACP96 C*	*ACP96 τ*	W_{IRIS}-W_{ACP96} Average	W_{IRIS}-W_{ACP96} Std Dev	W_{IRIS}-W_{ACP96} Max	W_{IRIS}-W_{ACP96} Min
W_{IRIS2}-W_{ACP96}	18802	10.72	0.9820	0.04	1.08	3.90	-4.24
W_{IRIS4}-W_{ACP96}	14085	10.28	0.9707	-0.03	0.96	2.30	-3.37
W_{IRIS2}-W_{ACP96}	18802	*10.50*	*0.9764*	-1.19	1.44	2.42	-5.68
W_{IRIS4}-W_{ACP96}	14085	*10.50*	*0.9764*	-1.39	1.07	1.00	-4.84

If the three C values in Table 4 are converted to equivalent PSP F3 thermopile solar C_{solar} values it results in values centred on 9.35 +/- 0.3.

The process was repeated but using a convection coefficient γ of 6.5, with the results are presented in Table 5. The standard deviations and range of differences increase slightly when compared to the values derived using 8.4 for the convection coefficient. The resultant C values were reduced by 0.2, while the transmission values are reduced by ~0.0013.

Table 5. The statistics of (W_{IRIS}-W_{ACP96}) using ε_c=0.0225 and γ=6.5 from March to November 2020, for pairs of C and τ, that minimized the standard deviation of the (W_{IRIS}-W_{ACP96}). The difference statistics using the average C and τ of the IRIS2 and IRIS4 results are also given in the last two rows of the table.

	No	*ACP96 C*	*ACP96 τ*	W_{IRIS}-W_{ACP96} Average	W_{IRIS}-W_{ACP96} Std Dev	W_{IRIS}-W_{ACP96} Max	W_{IRIS}-W_{ACP96} Min
W_{IRIS2}-W_{ACP96}	18802	10.51	0.9819	0.08	1.41	3.67	-4.39
W_{IRIS4}-W_{ACP96}	14085	10.06	0.9692	-0.04	0.99	2.23	-3.28
W_{IRIS2}-W_{ACP96}	18802	*10.28*	*0.9756*	0.19	1.43	3.71	-4.06
W_{IRIS4}-W_{ACP96}	14085	*10.28*	*0.9756*	-0.03	1.04	2.32	-3.38

The results in Tables 4 and 5 indicate that a negative 22% change in the convection coefficient reduces C by 2% and increases the transmission by 0.1% to achieve mean irradiance differences less than 0.1 Wm^{-2}. These changes are self-consistent given the high correlation between the components of the ACP equations either of Reda et al., 2012 or the new equation and shows a 2 Wm^{-2} impact with a change in the convection component of 1.9. However, for the averaged values of C and transmission the lower convection coefficient provided the averages closest to zero for both reference irradiance. The transmissions in Table 4 and 5 from using the mean of the IRIS2 and IRIS4 results are within 0.002 of the 0.977 value derived for ACP95 using the new equation and NIST laboratory measurements (Zeng et. al., 2010).

The small differences (W_{IRIS2}-W_{IRIS4}) for two days in August and the high correlation between components in the new equation demonstrates that uncertainty in the reference irradiance impacts the minimization method and shows the benefit of having multiple reference irradiances to assess confidence intervals.

The increase in C with an increase in transmission and the magnitude of these changes is a consequence of the difference in the measured W_{IRIS2} and W_{IRIS4}. The two dominant components of W_{atm} using the new equation, are the thermopile voltage and the thermopile blackbody irradiance W_r; the contributions from W_c and (T_r - T_c) are less than 4%. The magnitude of the irradiance derived from the thermopile signal is of the order of -80 Wm^{-2} while W_r is typically between 300 and 500 Wm^{-2}. Hence if the minimization method is to achieve a balance between K_1 and transmission, for a 1 Wm^{-2} change in reference irradiance, then K_1 changes by the higher percentage as the W_r is unchanged. If only K_1 was minimized instead of a (K_1, τ) pair, then a Δ Wm^{-2} difference in W_{atm} would result in K_1 changing by Δ/W_r. Further complications arise if the relationship between the true W_{atm} and W_{ref} changes.

8.4 Adaption of Reda et al., 2012 linear LSQ calibration method to the new equation

From Eq. (18) and assuming the fraction of backscatter of incoming irradiance β is zero we can define the predictand for the linear LSQ analysis as

$$y(W_r, W_c, T_r, T_c, t) = W_{net}(t) = W_r(t) - \varepsilon_c W_c(t) + \gamma(T_r(t) - T_c(t)) \quad (25)$$

with the thermopile voltage V the predictor for the linear LSQ analysis, hence the equation to solve by linear LSQ is

$$y(W_r, W_c, T_r, T_c, t) = W_{net}(t) = <\tau W_{atm}> - <K_1> V(t) \quad (26)$$

which results in a $<C> = 1/ <K_1>$ and is independent of concentrator transmission. From $<\tau W_{atm}>$ by assuming a value for the concentrator transmission results in values for $<W_{atm}>$ which could be compared to a reference irradiance. The inverse would be to prescribe a reference irradiance and derive a concentrator transmission.

For the linear LSQ process to be successful, W_{atm} and γ must be constant during the data collection process and the ACP equation must be valid. In stable W_{atm} conditions, the process for collecting the required rapid cooling periods results in only small changes in T_c and W_c. As a result, the changes in concentrator irradiance component $\varepsilon_c W_c$ are less than 0.1 Wm^{-2} over the entire rapid cooling process, and hence minimal impact on $<K_1>$.

Given the properties of linear LSQ, using a single predictor, $V(t)$, if the predictand is made up of multiple linear components one can solve for each component of the predictands independently. The three predictand components from Eq. (18) are

$$W_r(t) = y_r(t) = <A_r> V(t) + <B_r> \quad (27)$$

Similarly

$$W_c(t) = y_c(t) = <A_c> V(t) + <B_c> \quad (28)$$

and lastly

$$dT(t) = \left(T_r(t) - T_c(t)\right) = y_{dT}(t) = <A_{dT}> V(t) + <B_{dT}> \quad (29)$$

d$T(t)$ can also be split into three separate components, but that will be left to the discussion section of this paper on the impact of incorrect estimates of the Seebeck coefficient and assuming $T_c(t)$ is equivalent to $T_{air}(t)$.

Derived $<K_1>$ and $<\tau W_{atm}>$ using the new equation are given by

$$<K_1> = <\frac{1}{C}> = \varepsilon_c <A_c> - <A_r> - \gamma <A_{dT}> \quad (30)$$

and

$$<\tau W_{atm}> = <B_r> - \varepsilon_c <B_c> + \gamma <B_{dT}> \quad (31)$$

Given W_c is almost constant through the ~7 minute cooling of the thermopile, and $|<A_c>|<0.005$, then $|\varepsilon_c<A_c>| < 0.00015$ and contributes less than 0.1% to $<K_1>$, hence the concentrator emissivity has minimal impact on deriving $<K_1>$ using the new equation. For the intercept terms $\varepsilon_c<B_c>$ typically makes a small negative contribution to $<\tau W_{atm}>$ of the order of 2.5%. W_r and $(T_r\text{-}T_c)$ dominate contributions to both $<K_1>$ and $<\tau W_{atm}>$.

The concentrator transmission is irrelevant to deriving $<\tau W_{atm}>$ or $<K_1>$ but is essential for estimating $<W_{atm}>$ from $<\tau W_{atm}>$. If W_{atm} is known through a reference radiometer (W_{ref}), then the concentrator transmission can be estimated by

$$\tau = \frac{<\tau W_{atm}>}{W_{ref}} \quad (32)$$

For any linear LSQ process there is a key requirement that the process is linear, and for Eq. (18) τW_{atm} must be constant. As a result, initial criteria for acceptable conditions were established for a valid linear LSQ analysis period.

When the base of the ACP is cooled rapidly, the thermopile signal must continuously become less negative. As the thermopile voltage was measured every 10 seconds, a valid time was defined when the following criteria were met: (a) the difference in consecutive thermopile voltages was more than +3.5 μV; (b) the difference in consecutive ($T_r(t)$-$T_c(t)$) to be less than -0.04 K. (c) the total range of the voltage was greater than 200 μV; and (d) (T_r-T_c)(t_i)-(T_r-T_c)(t_{i-1})<0.02. These ensured the cooling was not nearing the new base temperature or that cooling had stopped.

Out of 266 possible periods during 2020 for ACP96, 244 linear LSQ calibration periods satisfied the criteria. Figures 5 through 6 show the time series of the individual slopes <A_c>, <A_r>, <A_{dT}>, and intercepts (<B_r>, <B_c>, <B_{dT}>) derived from the valid linear LSQ analyses. <A_c>, <A_r> are stable about a mean value but the slopes for (T_r-T_c), and <A_{dT}>; meteorological data for these periods indicates the dew point temperature was less than 4 K below the ambient temperature and thermopile surface temperatures during cooling were close to or less than the dew point. While <B_{dT}> is relatively constant over the year, as expected <B_r> and <B_c> follow the irradiance of the ambient temperature peaking in summer periods.

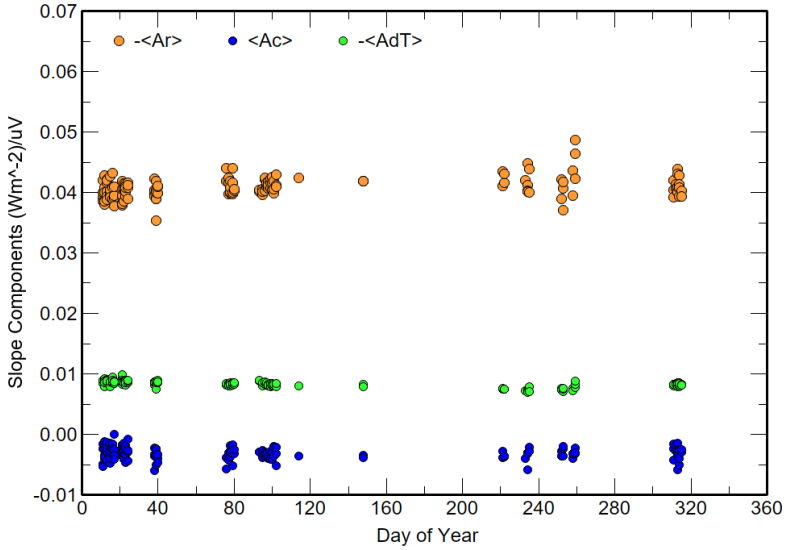

Figure 5. The linear LSQ slope <A_r>, <A_c> and <A_{dT}> components that generate <K_1> for 244 calibrations in 2020.

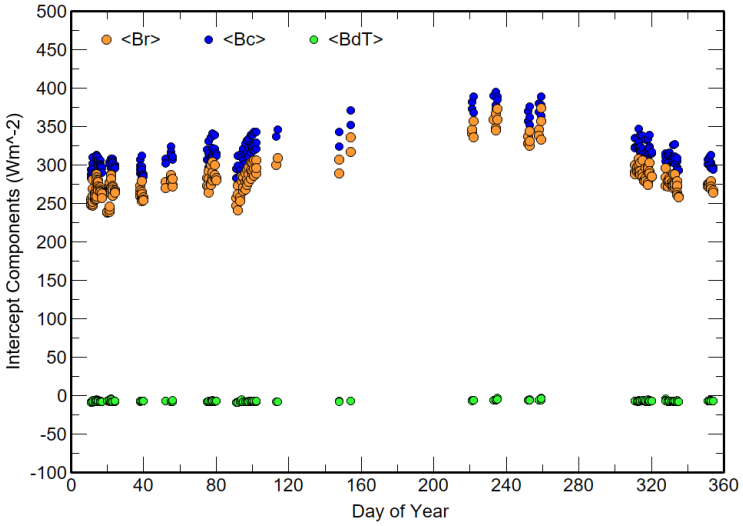

Figure 6. The linear LSQ slope <B_r>, <B_c> and <B_{dT}> components that generate <τW_{atm}> for 244 calibrations in 2020.

The thermopile responsivities <*C*> found for 244 linear LSQ calibration periods are shown in Figure 7. Between days 210 and 260 there is a significant increase in the range of <*C*>, compared to the rest of the year.

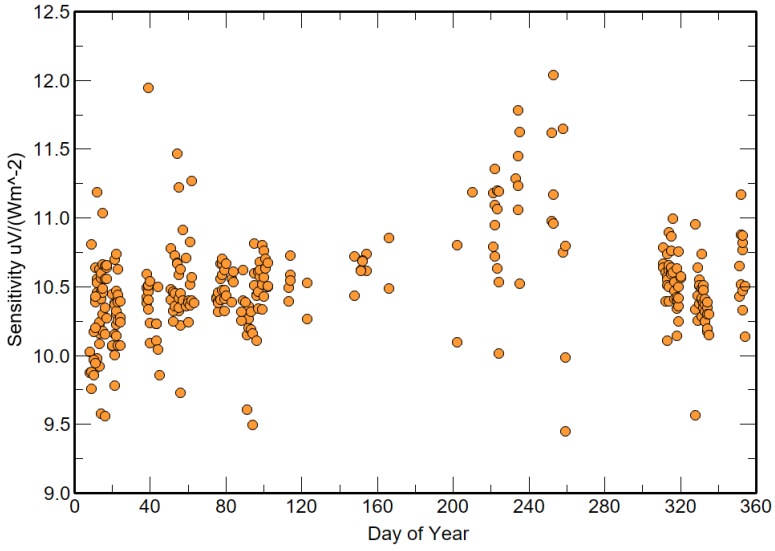

Figure 7. ACP96 <*C*> values derived using the new equation using the linear LSQ method with ε_c = 0.0225, γ=6.5 for 244 calibration periods in 2020.

There were 115 periods that were coincident with IRIS2 measurements when the standard deviation of W_{IRIS2} in a cooling sequence was less than 0.4 Wm^{-2} and 63 coincident with IRIS4 also with a standard deviation less than 0.4 Wm^{-2}. <*C*> statistics for the 244 linear calibration periods and irradiance differences for the coincident periods with W_{IRIS2} or W_{IRIS4} are presented in Tables 6 and 7 for γ=6.5 and γ=8.4 respectively.

Table 6. Linear LSQ method results for ACP96 <*C*> using ε_c = 0.0225, γ=6.5 and τ=0.977 and the difference between ACP96 and IRIS irradiances when coincident data were available (W_{IRIS} - <W_{atm}>). <*C*> statistics for the entire 244 linear LSQ calibrations are presented in the first data row. The 2nd and 3rd data rows concern periods when ACP96 and IRIS 2 data were available; the 4th and 5th data rows concern periods when ACP96 and IRIS4 were available. The last data row gives the statistics of the irradiance differences between the two IRIS for 63 days of coincident data.

Parameter	Mean	N	σ	Max	Min
<*C*>	10.49	244	0.36	12.04	9. 45
σ_{IRIS2}<0.4 Wm^{-2}					
<C>	10.47	115	0.25	11.42	9.98
W_{IRIS2}-<W_{ACP}>	-0.04	115	2.23	3.98	-6.85
σ_{IRIS4}<0.4 Wm^{-2}					
<*C*>	10.58	63	0.26	11.42	10.01
W_{IRIS4}-<W_{ACP}>	-1.19	63	1.80	2.76	-5.83
W_{IRIS2}-W_{IRIS4}	0.69	63	1.12	2.94	-1.30

Table 7. Linear LSQ method results for ACP96 <*C*> using ε_c = 0.0225, γ=8.4 and τ=0.977 and the difference between ACP96 and IRIS irradiances when coincident data were available (W_{IRIS} - <W_{atm}>). The 1st and 2nd data rows concern periods when ACP96 and IRIS 2 data were available; the 3rd and 4th data rows concern periods when ACP96 and IRIS4 were available.

Parameter	Mean	N	σ	Max	Min
σ_{IRIS2}<0.4 Wm^{-2}					
<C>	8.58	115	0.26	9.75	7.90
W_{IRIS2}-<W_{ACP}>	13.16	115	3.20	17.92	2.16
σ_{IRIS4}<0.4 Wm^{-2}					

$<C>$	8.70	63	0.28	9.75	8.21
W_{IRIS4}-$<W_{ACP}>$	11.68	63	2.95	17.28	2.47

The differences (W_{IRIS2}-$<W_{atm}>$) and (W_{IRIS4}-$<W_{atm}>$) for coincident measurements using a convection coefficient of 6.5 are shown in Figure 8. The results between days 200 and 254 for both $<C>$ and the $<W_{atm}>$ appear anomalous with significantly higher values of $<C>$ and underestimates of the irradiance differences; these are during periods when the steady state base temperature is typically high for the year and within 4 K of the dew point temperature and high relative humidity of 80%. The means of pre day 200 and post day 300 are separated by about 2.2 Wm^{-2}. Given that $<C>$ is likely constant over the two periods possible reasons for the 2.2 Wm^{-2} irradiances are: (i) both reference IRIS irradiances calibration may have changed by the same amount; (ii) the transmission of the concentrator may have decreased; (iii) the use of a constant convection coefficient over the entire year is inappropriate.

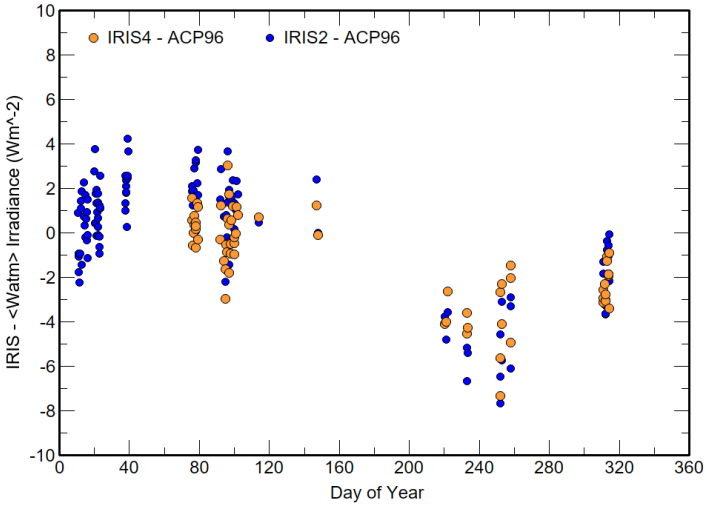

Figure 8. Daily mean irradiance differences (W_{IRIS} - $<W_{atm}>$) between the mean IRIS (W_{IRIS}) and linear LSQ interpolated ACP96 ($<W_{atm}>$), using the new equation with ε_c = 0.0225, γ=6.5, and τ = 0.977.

The mean derived $<C>$ value in Table 5 using 6.5 as the convection coefficient is 10.49 µV/(Wm^{-2}) which is within 0.3 µV/(Wm^{-2}) of the solar and minimization methods. Table 7 using the higher convection coefficient of 8.4 shows a mean C about 18% lower and the irradiance differences greater than 11 Wm^{-2} between the ACP96 and IRIS2 and IRIS4.

No attempt was made to adjust the concentrator transmission τ based on the derived $<C>$ (or K_1), as it is a property of the concentrator not the thermopile. However, it was possible to estimate τ using the derived $<\tau W_{atm}>$ from the linear LSQ intercept which is independent of any assumed value of τ by dividing $<\tau W_{atm}>$ by W_{IRIS4}.; similarly, the derived $<\tau W_{atm}>$ from the Reda

et al., 2012 equation could also produce an estimate of the concentrator transmission τ. Figure 9 shows the results of dividing the $<\tau W_{atm}>$ derived from both LSQ equations by IRIS4 data. Similar results were obtained using $W_{IRIS2.}$ The results using the new equation suggest a concentrator transmission τ~0.98, while for the Reda et al., 2012 equation a significant majority of periods gave unphysical values of τ greater than 1.

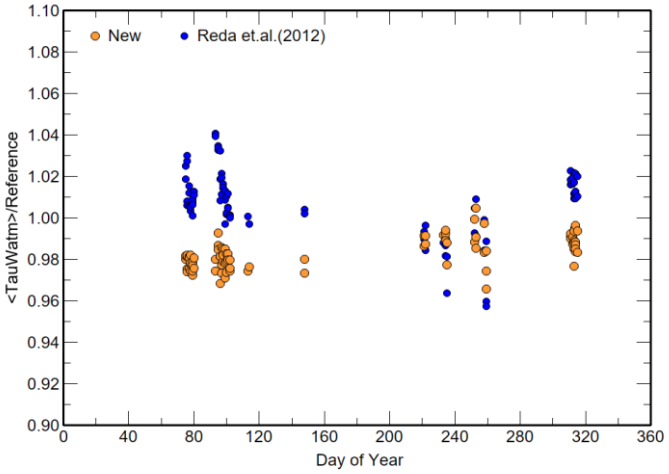

Figure 9. Concentrator transmission estimates derived from dividing the linear LSQ obtained $<\tau W_{atm}>$ by W_{IRIS4} for 63 estimates using the new equation (18) and the Reda et. al. (2012) equation (22) estimate of $<\tau W_{atm}>$.

8.5 Ensuring the representativeness of τW_{atm} during a linear LSQ calibration period

The thermopile voltage measurement is a consequence of net irradiance based on the temperature difference between the base of the thermopile to the top of the thermopile. The black body equivalent irradiance of the thermopile receiver is calculated by assuming the Seebeck coefficient is valid and the body temperature represents the temperature at the base of the thermopile. Provided the time constants of the thermopile and thermistors are similar and the heating or cooling of the body are not too rapid, C and the convection coefficient should provide τW_{atm} for all measurements (or K_1 Eq. (22)) and ideally produce a near constant value during both cooling and heating.

Using the data for ACP96 in 2020, and the calculated mean values of C given in Table 6, $\tau W(t)$ was generated for each cooling and heating period. $\tau W_{atm}(t)$ was found to maintain some repeatable oscillations that could not be minimized by changing either the convection coefficient or C for the new equation. For the Reda et al., 2012 equation only K_1 could be varied and resulted in decreases of calculated irradiances over the cooling and heating period regardless of the K_1 used with little if any impact on deviations from a presumably constant τW_{atm}.

The sinusoid shape of the oscillation in the derived τW_{atm} using Eq. (18) gave higher values during cooling and lower values during heating, suggested that there was a phase difference between the thermopile voltage and the body temperature or some processes unaccounted for using the new equation. If a phase issue, the thermopile voltage at measurement period p was lagging the changing body temperature, and hence the temperature of the body at time t was not representing the temperature of the thermopile base at t. Such differences would be tiny in steady state conditions given the slow rate of change in T_b.

Linear interpolation in time was used to find a more representative thermopile voltage that reduced the sinusoidal oscillation in the derived τW_{atm} and found that for ACP96 a lag time of about 9 s +/- 2 s was required to reduce the magnitude of oscillations about the mean when using the new equation τW_{atm}. It also reduced the magnitude of the difference from the constant τW_{atm} using the Reda et al., 2012 equation but a distinct sinusoid always remained with peak deviations of 2 Wm^{-2} or more but 180 degrees out of phase with the new equation values.

Given measurements for all quantities were repeated every 10 s, the most representative thermopile voltage for measurement p every 10 s, $V_{p'}$ was

$$V_{p'} = V_p + 0.9\,(V_{p+1} - V_p) \quad (33)$$

Using this interpolated voltage $V_{p'}$ to represent the thermopile voltage at p, resulted in significantly improved standard errors and confidence intervals for each of the linear LSQ derived components of $<K_1>$ and $<C>$ by factors of 3 to 10 depending on the linear LSQ component and provided statistics for the variation of τW_{atm} throughout each cooling and heating period. The improved linear LSQ fits did not impact significantly on the derived $<K_1>$ or $<C>$ only raising $<C>$ by less than 0.02, with no significant difference to the results presented in section 8.4.

Using equation (33) to represent the thermopile signal for measurement p and setting a maximum standard deviation limit of τW_{atm} over the cooling and heating period of 0.6 Wm^{-2} as acceptable when using the new equation, the results for $<C>$ derived by linear LSQ in section 8.4 were re-examined. Figure 10 shows the same $<C>$ values as in Figure 7 and those that satisfy the standard deviation of τW_{atm} criterion. Of the 244 original values, only 51 had larger standard deviation in τW_{atm} over the cooling period. The main impact of this limit was removal of outliers. It had little impact on the divergence of results between days 200 and 260 in 2020.

The phase shift showed that both the new and Reda et.al., 2012 equations could represent τW_{atm} through the cooling and heating with varying degrees of success. A cumbersome visual method showed that varying the convection coefficient constant for each cooling-heating cycle further reduce the size of the deviations from τW_{atm} by was not independent of the estimate for C but is not the subject for this current paper. Most importantly, automation of the visual method may provide a method of judging if τW_{atm} was nominally constant during a linear LSQ calibration period and thus remove the requirement of a reference radiometer for that purpose.

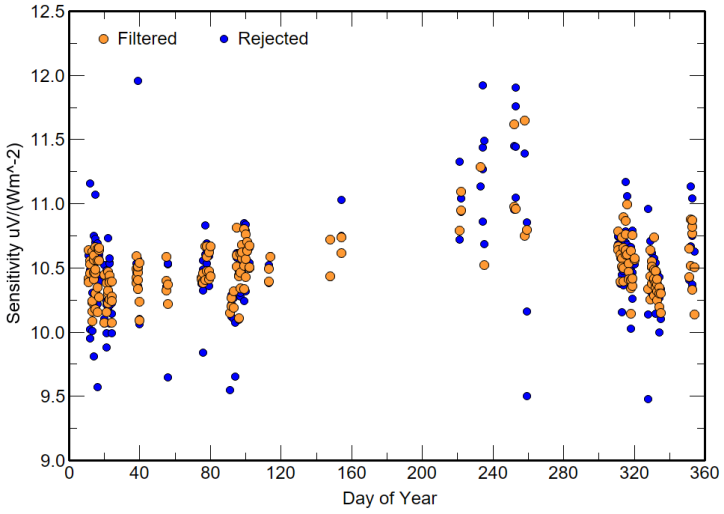

Figure 10. Responsivity <*C*> values presented in figure 7 but filtered for standard deviations of ACP96 τW_{atm} during the cooling-heating period that are less than 0.6 Wm^{-2} are gold, and those with higher standard deviations are in blue.

9 Discussion

The four different methods using the new ACP irradiance equation to calibrate the ACP96 provided irradiances that compared well with the irradiances from IRIS2 and IRIS4 during 2020. One was based on laboratory or blackbody estimates for concentrator emissivity, transmission and the convection coefficient provided an estimate of *C* based on the modal value over 80 new F3 thermopile solar calibrations. Another used minimization of the differences between the ACP and IRIS radiometers for pairs of *C* and concentrator transmission. The third used the new equation with the linear LSQ of Reda et al., 2012 but treated every contributor separately. The fourth used the derived calibrations in third method to estimate τW_{atm} from every measurement during a cooling and heating period and thereby filter the results for stable periods without the need for a separate pyrgeometer. All methods produced mean differences from IRIS2 and IRIS4 less than 1.2 Wm^{-2} and typically ranges of +/-3 Wm^{-2} from the mean difference for IRIS4. The differences in irradiances between IRIS2 and ACP96 were not symmetric about the mean, suggesting an identical trend in calibration of either both ACP96 and IRIS4 simultaneously or just IRIS2. As the year progressed the daily mean differences between IRIS2 and ACP96 became increasingly negative until day 300 when irradiances recovered and equated to IRIS4 as during March and April 2020.

That the pseudo solar calibration method produced a value very close to the other methods was fortuitous given that it was based on the modal value of initial PSP calibrations based on 82 instruments. The range of potential values matched the derived results and suggests that a solar calibration of the ACP F3 thermopile is both a useful first step in characterising an ACP

thermopile as well as estimating the maximum potential ACP *C* calibration and the method could be used periodically to check the stability of the thermopile. An extended solar calibration over ambient temperature ranges using the method of Pascoe and Forgan (1980) could also confirm the temperature compensation of the thermopile. However, given the decadal decrease in responsivity of the F3 thermopiles in PSP radiometers, exposure of an ACP thermopile to solar exposure should be kept to a minimum to reduce the impact of solarization of the Parsons Black paint. Using the solar method as a primary calibration also negates the ACP as an absolute irradiance reference standard as well as being based on historical estimates of the emissivity of Parsons Black in both the IR and solar wavelengths. However, as most World Meteorological Organization regional instrument centres have ready access to well-maintained reference pyrheliometers but do not have laboratory facilities to characterize the concentrator, solar calibrations could be a useful verification and monitoring tool. At a minimum, the solar calibration will provide a lower limit for K_1 (and hence an upper limit for *C*). That the theoretical value derived from the nominal solar calibration from an ensemble of new PSP F3 thermopiles gave mean deviations of less than 1.5 Wm^{-2} for over 14000 measurements with a standard deviation of ~1 Wm^{-2} supports this recommendation.

The second method used an IR reference irradiance using IRIS pyrgeometers to solve for both *C* and concentrator transmission simultaneously. The reference pyrgeometers, both IRIS, are not influenced by calibration coefficients dependent on the spectral transmission and emission of IR of the domes. However, it was clear from the 2020 comparison data that any reference radiometer must have an up-to-date calibration, with distinct steps and trends in the derived relationship between the ACP and IRIS radiometers in the comparison data. However, irradiance differences are all well within the current WMO traceability requirement for terrestrial irradiances of 5 Wm^{-2}.

The concentrator transmission derived for ACP95 using the data from Zeng et. al. (2010) but the new equation, and the NIST value of concentrator emissivity reported by Reda et al., 2012, were applied to ACP96 and produced good agreement with the IRIS2 and IRIS4 measurements regardless of the methods described above. This suggests that these parameters could be used as a first approximation for any ACP. If an ACP is to be used without reference to a blackbody or reference radiometer, the concentrator emissivity should be obtained independently in the laboratory using the laboratory techniques reported by Reda et al., 2012 and the impact of a significant error in the emissivity for any irradiance calculation by the new equation would be small. However, as the difference between the true versus assumed concentrator transmission will have a directly proportional effect on W_{atm}, an alternative method to obtain the concentrator emissivity would be to repeat the Zeng et al., 2010 methodology for each ACP using the new equation to generate a concentrator transmission and then assume the emissivity is (1-τ).

By deriving τW_{atm} from each measurement in a cooling and heating calibration period the phase lag between the cooling of the base and the base of the thermopile became clear. The distance between where the base temperature is measured and the base of the thermopile is about 10 mm, and during the calibration periods the delay in response of the thermopile base was found to be about ~9 s for ACP96. Including that phase lag in the linear LSQ methods improved the confidence intervals for each linear LSQ analysis by factors of 3 to over 10 but had little impact on the derived gradients and intercepts. However, it did

improve the measurement estimate of τW_{atm} from individual measurements and provided a method to estimate the variance of τW_{atm} during a calibration period without need of a reference radiometer.

The comparisons between the IRIS and ACP irradiances in the results above suggest that the ACP thermopile was stable over the year and produced irradiance ratios to a reference within 2% over 2020 and with maximum differences of 5 Wm^{-2}. Reda et al., 2012 stated that the linear LSQ $<K_1>$ value from a single linear LSQ calibration period be used as the valid sensitivity for the period between the end of the heating period that generated the linear LSQ value until the next LSQ calibration period usually within three hours. The results from Reda et al., 2012 and the results presented above for ACP96 suggest that during a single night of linear LSQ calibrations the derived $< K_1>$ can vary by more than ±5% yet the typical F3 thermopile is found to be stable well within ±2% over years for both solar and IR measurements. In other radiometric linear LSQ calibration methods mean or mode statistics of several linear LSQ calibrations are used to reduce uncertainty in calibrations on the assumption that $<C>$ is a constant. The results above support using a C that represents a mean or mode resulting from more than 20 calibration periods spread over several nights.

9.1 Uncertainty in the Seebeck coefficient using linear LSQ

The equation from Reda et al., 2012 and the new equation are dependent on the estimate of the Seebeck coefficient S in Eq. (7). A fixed value of 7.044×10^{-4} was used in the analysis above. In steady state conditions when measuring the incoming irradiance, the impact of any offset from the true value is likely minor provided the other coefficients in new equation are have low uncertainties.

The Seebeck coefficient has direct influence in both the W_r term and the $(T_r\text{-}T_c)$ term of the new equation. For the $(T_r\text{-}T_c)$ term the impact is straight forward given Eq. (7) in that if the error in the Seebeck coefficient is ΔS then the contributory error is $\Delta S\gamma$ for $<K_1>$ and $<\tau W_{atm}>$. The impact of any error in S is slightly more complicated for W_r but the ACP96 2020 data suggest similar impacts. This is shown in Figure 11 plotting the difference in $<K_1>$ when ignoring S in the $<A_r>$ term. The difference was calculated by subtracting the receiver slope assuming S=0, that is base irradiance slope $<A_b>$, from the slope derived using S. The difference changes through the year inversely to the magnitude to the base temperature, but on average is ~-0.0033 or about -4% of $<K_1>$ which implies a 25% error in S has an impact of 1% on $<K_1>$.

For the Reda et al., 2012 equation the impact of the Seebeck coefficient is nearly doubled as the scaling factor is $(2\text{-}\varepsilon_c)$ instead of 1 for the new equation.

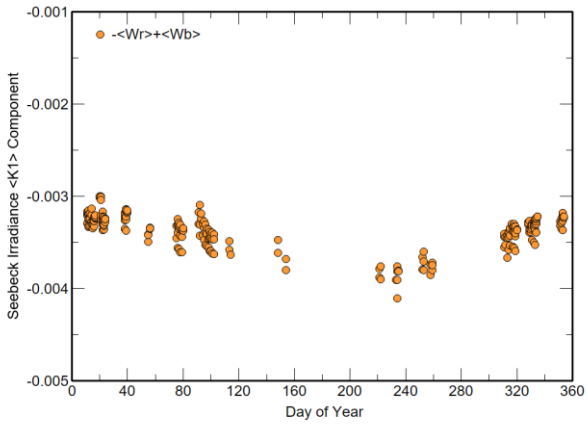

Figure 11. The difference in the receiver irradiance slope <A_r> and the slope by assuming the Seebeck coefficient is zero <A_b>when deriving <K_1> from the linear LSQ slope.

9.2 Comparing <C> and <τW_{atm}> using the Reda et al., 2012 equation and the new equation.

Isolating the coefficients that impact on the derived < K_1> via linear LSQ also allows the calculation of the <K_1> value based on the Reda et al., 2012 equation. Figure 12 shows the two components in Eq. (22) after applying the scaling factors to generate <K_1>; in essence W_r dominates the calculation with a small negative contribution from W_c.

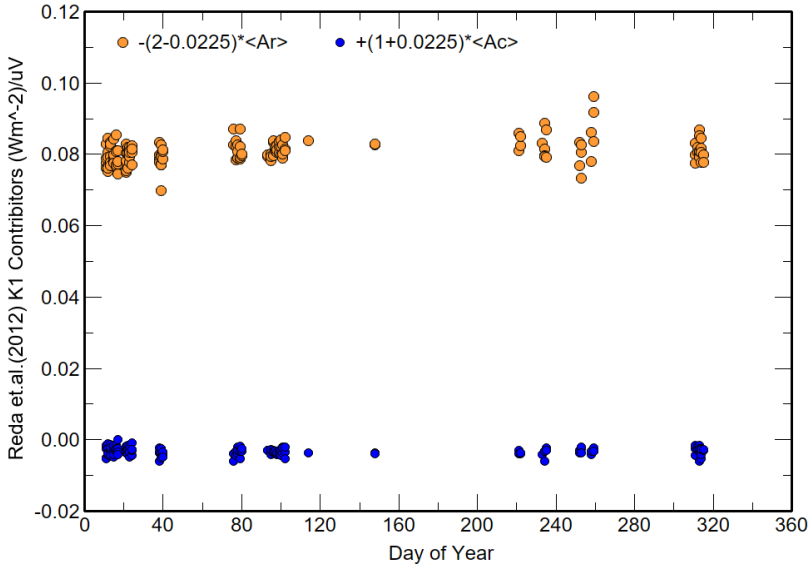

Figure12. The two slope contributions to < K_1> for the equation developed by Reda et al., 2012.

The differences between the derived <*C*> for both the new and Reda et al., 2012 equations by linear LSQ are shown in figure 13 and for <W_{atm}> in figure 14. The different types of <*C*> are separated by about 2.5 uV/(Wm^{-2}) with the Reda et al., 2012 values being higher. The <W_{atm}> differences between IRIS4 and Reda et al., 2012 equation were between +/-12 Wm^{-2}, while the differences to the new equation are bounded by +4 and -8 Wm^{-2} about half the range of the Reda et al., 2012 equation results.

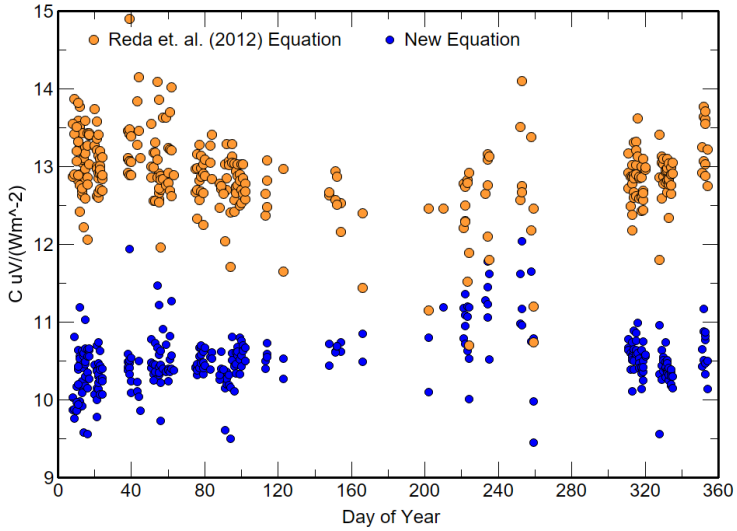

Figure 13. The derived *C* values derived from 244 linear LSQ calibration in 2020 for the Reda et al., 2012 and new equation using and concentrator emissivity of 0.0225 for both and a convection coefficient of 6.5 for the new equation.

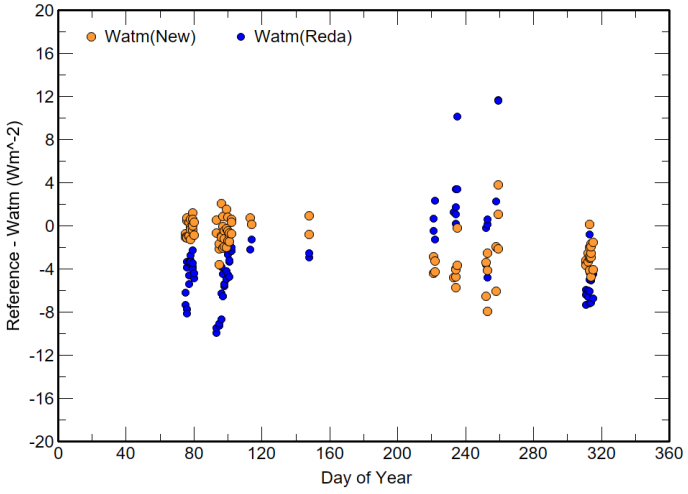

Figure 14: The comparison of <W_{atm}> derived from the new and Reda et al., 2012 equations to the mean IRIS4 irradiances for each linear LSQ calibration period in 2020.

9.3 Uncertainties in concentrator emissivity and convection coefficient

Three coefficients related to the concentrator are required for Eq. (18) to derive ambient irradiances and use the LSQ method of calibration. Zeng et. al. 2010 provided a laboratory method for determining the transmission and an estimate of its uncertainty, but laboratory determinations of the emissivity and convection coefficient have not occurred.

The W_{atm} uncertainty estimates in Table 1 indicate that the incorrect assignment of the convection coefficient γ has a minor contribution on the calculation of W_{atm} even if the coefficient's standard uncertainty is 25% from the true value. However, the emissivity is the second largest contributor to uncertainty after thermopile calibration coefficient in the determination of W_{atm}.

Table 8 provides an assessment of the uncertainty of the derived components of the linear LSQ method for the new equation. For this analysis the uncertainties of the voltage signals are simply the estimate of the signal resolution, and the derived calibration constant incorporates any proportional uncertainty in the true voltage. The uncertainties of the receiver and concentrator irradiance are incorporated in LSQ slope and intercept statistics, as are the uncertainties of the differences between the receiver and the assumed air temperature.

In Table 1 the uncertainty of the convection coefficient was 1.5, but in Table 8 it is 0.3. Even after reducing the uncertainty component for the convection coefficient by a factor of 5 from that used in Table 1 this coefficeint is the dominant contribution to the standard uncertainty of the derived <K_1>, and is close to the dominant uncertainty contribution from the receiver irradiance <B_r> for the estimate of <τW_{atm}>.

The convection coefficient of air is dependent on the design of the air flow path and temperature, with higher water vapour content also giving a higher coefficient. Empirical models of convection for the ACP are yet to be developed to determine the non-dimensional Nusslet parameter necessary for assigning and estimate of the convection coefficient.

The new equation was developed applying Kirchhoff's law of radiative transfer for radiative transfer in air. For the solar calibration method and the calibration using a reference irradiance, the ACP is essentially in steady state, while in the linear LSQ method the ACP is in a transient mode. Kirchhoff's law only applies in periods of radiative equilibrium, and this must be considered when modifying the cooling and heating cycle for linear LSQ calibrations.

Table 8. The standard uncertainty calculation for <K_1>, <τW_{atm}> and <W_{atm}> by linear LSQ regression of Eq. (18). The units of slope components (<A_x>) are $Wm^{-2}/\mu V$, while the intercept components are Wm^{-2}.

Component x	Value	dx (u_{66})	dW/dx	dx*dW/dx	$(dx*dW/dx)^2$

$<K_1>$					
$<A_r>$	-4.12x10-2	1	$7.56x10^{-4}$	$7.56x10^{-4}$	$5.72x10^{-7}$
$<A_c>$	$-3.36x10^{-3}$	0.0225	$7.80x10^{-4}$	$1.76x10^{-5}$	$3.08x10^{-10}$
ε_c	0.0225	$2.25x10^{-3}$	$-8.89x10^{-3}$	$-7.56x10^{-7}$	$5.72x10^{-13}$
$<A_{dT}>$	-8.89x10-3	6.5	$1.62x10^{-5}$	$1.05x10^{-4}$	$1.11x10^{-8}$
γ (Wm^{-2}/K)	6.5	-8.89x10-3	0.3000	$-2.67x10^{-3}$	$7.11x10^{-6}$
				$\Sigma(dx*dW/dx)^2$	$7.70x10^{-6}$
			$<K_1>$	Std. Uncertainty	0.0028
$<\tau W_{atm}>$					
$<B_r>$	260.2	1	2.50	2.50	6.25
$<B_c>$	294.18	0.0225	2.58	$5.08x10^{-2}$	$3.36x10^{-3}$
ε_c	0.0225	294.18	0.000225	0.662	0.438
$<B_{dT}>$	-7.95	6.5	0.204	1.33	1.76
γ (Wm^{-2}/K)	6.5	-7.95	0.3	-2.39	5.59
				$\Sigma(dx*dW/dx)^2$	14.14
			$<\tau W_{atm}>$	Std. Uncertainty	3.76
$<W_{atm}>$					
τ^{-1}	1.0235	282.685	0.005	1.413	1.998
$<\tau W_{atm}>$	260.68	1.2035	3.76	3.848	14.81
				$\Sigma(dx*dW/dx)^2$	16.81
			$<W_{atm}>$	Std. Uncertainty	4.10

9.4 Future Work

While the investigations above demonstrate that the new equation can be used with an ACP for terrestrial irradiance measurements and give good agreement with pyrgeometers with traceability to SI, there are still uncertainties related to the new equation and the characteristics of ACP pyrgeometers to be suitable direct references to SI irradiances. For example, a significant issue is how the Reda et. al. 2012 and the new equation Eq. (18) can produce valid terrestrial irradiances but utilize thermopile sensitivities that differ by 25% or more.

While the uncertainty in the convection coefficient has little impact on calculating outdoor irradiances, it is the dominant uncertainty when using the linear LSQ method for calibration with the new equation. The following are future actions recommended to increase confidence of ACPs to act as a primary reference to SI: a method for determining the convection coefficient; determine theoretical approximations of the ACP convection coefficient by developing an appropriate dimensionless Nusslet coefficient for the thermal and air flow characteristics of an ACP; determine if the ACP can be calibrated in a black body but with a different process to that used with domed pyrgeometers; higher frequency measurements in cooling and heating cycles to conform the time offset between the thermopile reacting to a temperature change in the ACP base temperature; investigate if the heating part of the LSQ data collection process can be used for LSQ analyses; and perform solar calibrations of the thermopile to determine an ACP's maximum possible thermopile responsivity.

10 Conclusions

The new equation for an ACP derived from the application of Kirchhoff's law and inclusion of a convection term provided irradiances that agreed with measurements from two reference IR radiometers over 11 months in 2020 assuming either a solar derived calibration or minimization method.

The linear LSQ method of Reda et al., 2012 was modified for use with new equation, and developed so that the impact of individual contributors to the linear LSQ process could be assessed. As the only LSQ predictor was the thermopile voltage the method allowed determination of 5 linear components independently of the Reda et. al., 2012 and new equation. This also provided an estimate of the relative contribution of each component to the calibration values and their uncertainty contribution.

The linear LSQ results indicated that the new equation irradiances were for most cases consistent with the two reference radiometer irradiances, but that consistency was dependent on the value of the convection coefficient. A method of examining the convection coefficient independent of a reference irradiance was developed by solving for τW_{atm} during cooling and heating periods and highlighted ~9 s time lag between the representative voltage for the body and concentrator temperature measurements. When the lag was incorporated into the linear LSQ method the confidence intervals for all slope quantities improved significantly and systematic variations in the derived irradiance during a heating cooling period were reduced but not eliminated. However, a process to determine the convection coefficient independent of outdoor or laboratory measurements has yet to be developed.

Via the linear LSQ method an estimate for the concentrator transmission can also be obtained using a reference terrestrial irradiance. However, the preferred method should be laboratory measurements as performed by Zeng et al., 2010 but using the new equation rather than assuming the measurements are performed in a vacuum.

A solar calibration of future ACP thermopiles is recommended provided the thermopile has not been subjected to solar irradiance for extended periods over several years. The solar calibration will produce an estimate of the thermopile responsivity that will be close to the maximum possible for the thermopile and thus provide either an independent estimate or a mechanism to assess the long-term stability of the ACP thermopile responsivity.

References

Gröbner, J.: A transfer standard radiometer for atmospheric longwave irradiance measurements, Metrologia, 49, 105-111, 2012.

Gröbner, J. and Wacker S.: Pyrgeometer calibration procedure at the WRC/PMOD-IRC, WMO, Instrument and Observing Report 120, pp13, 2012.

Gröbner, J., Investigation of ACP96 at PMOD/WRC, doi.org/10.5281/zenodo.7047680, 2021.

Kondratyev, Y. A.: Radiation in the Atmosphere. Academic Press, International Physics Series, Vol 12, pp 912, 1969.

Philipona, R., Frohlich C., Betz C.: Characterization of pyrgeometers and the accuracy of atmospheric long-wave radiation measurements, Appl. Opt., 34(9), 1598–1605, 1995.

Pascoe, D. and Forgan B. W.:(1980) An investigation of the Linke-Feussner pyrheliometer temperature coefficient, Solar Energy, 25, 191-192, 1980.

Robinson, G. D.: Solar Radiation, Elsevier, pp269, 1966.

Reda, I., Zeng, J., Hanssen L., Wilthan B., Myers D., T. Stoffel T.: An absolute cavity pyrgeometer to measure the absolute outdoor longwave irradiance with traceability to international system of units, SI. Jnl Atmos. Solar-Terrestrial Physics, 77, 132-143, 2012

Vignola, F., Michalsky J., T. Stoffel T.: Solar and infrared radiation measurements. CRC Press, ISBN 978-1-4398-5189-0, 2012.

Zeng J. Hanssen L., Reda I., Scheuch J.: Preliminary characterization study of a gold-plated concentrator for hemispherical longwave irradiance measurements. Paper no 77920Z. Proceedings of SPIE Conference -3-5 Aug 2010, San Diego Volume 7792. 2010.